SEDIMENTS, SEC 3 • HILLSLOPE AND RIVER BASIN SEDIMENT DYNAMICS • RESEARCH ARTICLE

Radionuclides and stable elements in the sediments of the Yesa Reservoir (Central Spanish Pyrenees):

Ana Navas • Blas Valero-Garcés • Leticia Gaspar • Leticia Palazón

A. Navas (✉) • L. Gaspar • L. Palazón
Estación Experimental de Aula Dei (EEAD-CSIC), Department of Soil and Water, Apartado 13034. 50080 Zaragoza, Spain
e-mail: anavas@eead.csic.es

B. Valero-Garcés
Instituto Pirenaico de Ecología (IPE-CSIC), Apartado 13034, 50080 Zaragoza, Spain

(✉) **Corresponding author:**
Ana Navas
Tel. 34 76 576511
Fax. 34 76 575620
e-mail: anavas@eead.csic.es

Abstract

Purpose: The sediments accumulated in the Yesa Reservoir (Central Spanish Pyrenees) have greatly decreased its water storage capacity and are a major threat to the sustainability of water resources in the region. The study examines the contents of radionuclides and stable elements in the reservoir sediments and relates their variations with the sediment composition and sedimentary dynamics, particularly flood frequency and intensity, responsible for changes in the main supply and distribution of radionuclides in the basin.

Materials and methods:. The sedimentary sequence accumulated in the The Yesa Reservoir (471 Hm^3) that supplies water for 1,000,000 population and irrigation was examined in two 4 m long sediment cores (Y1, Y2) and one profile (Y3) retrieved at its central part. In the sediments, radionuclide activities of ^{238}U, ^{226}Ra, ^{232}Th, ^{40}K, ^{210}Pb, and ^{137}Cs (Bq kg^{-1}) were measured using a hyperpure Ge coaxial detector. The stable elements Mg, Ca, Sr, Ba, Cr, Cu, Mn, Fe, Al, Zn, Ni, Co, Pb, Li, K and Na (mg kg^{-1}) were analysed by ICP-OES. Complementary analyses to characterize the sediments included: XRD in the profile, grain size distribution by laser equipment and contents of organic matter, carbonates and the residual fraction by loss on ignition.

Results and discussion: Variation in radionuclide activities is associated with grain size and sediment composition. The activity levels (Bq kg^{-1}) ranged between 20–43 for ^{238}U, 14–40 for ^{226}Ra, 7–56 for ^{210}Pb, 19–46 for Th^{232}, 1–48 for ^{137}Cs and 185–610 for ^{40}K. Enriched activity levels are associated with clayey and silty layers, and depleted levels with sandy layers. The levels of radionuclides and trace elements were significantly lower in the cores, than in the profile because of its higher silicate content and the influence of inflow of spring

mineral rich waters. The correlations among radionuclides, sediment components and stable elements evidenced stronger influence of the dynamic of sediment supplies by floods in the central areas closer to the main channel (cores) than in the littoral areas (profile).

Conclusions: The radionuclide distributions were consistent with the history of the reservoir infilling and with processes of transport and accumulation of sediments. Comparing with the natural radionuclides, the artificial ^{137}Cs varied the most and showed distinctive patterns. The methods used allow identification of natural inputs into the system and its differentiation from the fluvial transport and reservoir deposition. The results provide insights into the pathways and processes involved in the mobilization of radionuclides in the environment.

Keywords Gamma emitting • **N**atural and artificial radionuclides • Stable elements• Sedimentary sequence • Siltation • Yesa Reservoir • Spanish Pyrenees

1 Introduction

The sediments transported through a hydrological network and eventually accumulated in natural or man-made water bodies can affect the quality and sustainability of water resources. Each year, about 1% of the capacity of the world's reservoirs is lost because of infilling by sediments and this loss is a significant threat to the sustainability of water resources not only in semi-arid areas but at a global scale, considering that forecasted population growth will increase the water demand.

Reservoirs act as sinks for radionuclides and stable elements and, after being transported in dissolved or particle-associated forms, they remain trapped in different proportions in the sediments of reservoirs (e.g., McLean et al., 1991, Foster, 2006). The accumulation of fallout ^{137}Cs and excess ^{210}Pb generally exceeds the atmospheric loadings and estimates on their annual retention in three USA reservoirs ranged between ~15% and ~80% (McCall et al., 1984). Moreover, radionuclides in the sediments deposited at the bottom of reservoirs might affect water quality for human consumption (Callender and Robbins, 1993). Both, artificial and natural radionuclides are also found in lakes (Morellón et al., 2008; Valero-Garcés et al., 2008) and their impact on natural ecosystems dynamics has to be evaluated. Therefore, the presence of radionuclides in the materials that accumulate in water-bodies is an important environmental issue and requires the assessment of the mechanisms of radionuclide transport in fluvial networks and deposition in lakes and reservoirs.

The accumulation of sediments is a concern for most of the reservoirs in the Mediterranean region but, particularly, for those in mountainous areas, where high erosion rates and active sediment dynamics reduce rapidly the storage capacity of reservoirs. In 27 yr, the Yesa Reservoir on the Aragón River, Spain, has lost 21 Hm^3 of its storage capacity (CEDEX, Centro de Estudios y Experimentaciones). Most of the sediments arrive via storm events and, to a lesser extent, via snowmelt (Navas et al., 2008). The sediment loads deposited in the Yesa Reservoir are expected to affect the sustainability of water resources. Furthermore, a plan has been approved to double the initial water storage capacity of the reservoir and, for that reason, the nature of the stored sediments should be understood to contribute to the rational, sustainable use of water resources (Sundborg and Rapp, 1986). Hence, the characterization of sediments accumulated in reservoirs is necessary for the implementation of sediment mitigating strategies. Moreover, data on radiological and stable elements provide more extensive information required for the application of environmental conservation policies of water bodies.

In the past century, soil erosion from agricultural catchments have increased the amount of sediment supplies to water courses and changes in the sediment dynamics of catchments have been widely documented (e.g. Walling et al., 2003, Foster et al., 2007). In Mediterranean mountain headwaters impacts of land use changes have altered both runoff generation and sediment transport in the last decades (Navas et al., 2004) and thus the transfer of natural and artificial radionuclides linked to soil particles might have also been affected. The analysis of the vertical distribution of radionuclides and stable elements in sedimentary records of reservoirs can assist to identify the patterns of such changes. To improve the knowledge of the environmental behaviour of radionuclides and stable elements, a more detailed information of specific processes in reservoirs is required . In addition, an understanding of stable elements and their association with the radionuclides is helpful in identifying their patterns of mobilization and any common sources of potentially toxic elements (Jordan et al., 1997).

The concentration profiles of radioisotopes and elements in sediment cores from reservoirs aid in the identification of natural inputs, environmental changes, and artificial pollutants (Baeza et al., 2009). However, little is known about the radionuclide content, and vertical distributions thereof, in the sediments of reservoirs. In situ measurements should provide the ultimate information about the behaviour of radionuclide and stable elements of a particular ecosystem compartment such as reservoir deposits. This research examines the contents of radionuclides and other stable elements in the sediments that have accumulated at the bottom of the Yesa Reservoir (Aragón, Spain). The study based on a detailed analysis of the materials retrieved from two sediment cores and one profile collected from the submerged plains in the centre of the reservoir aims to provide insights into the pathways and the processes involved in the mobilization of the radionuclides in ecosystems. We also examined the relationships between the radionuclides and the general properties (grain size, organic matter, carbonates and silicate contents) of the sediments, the changes in sediment supply and the role of floods in the dynamics and transfer patterns of radionuclides and stable elements in Mediterranean mountain headwaters.

2 Materials and methods

2.1 The study area of the Yesa Reservoir

The Yesa reservoir, located in the Aragón River (Fig. 1), in an E-W elongated valley carved in easily eroded Tertiary sedimentary formations, is one of the largest in the Pyrenees (471 Hm^3) (Figure 1). The main inflow to the reservoir is supplied by the Aragón River (1019 Hm^3 per year). The reservoir was build in 1959 for irrigation of 60.700 has and recently also supplies water for the Zaragoza metropolitan area with around 1000000 inhabitants.

The basin drained by the Aragón river has an altitudinal gradient varying between 570 m to 2900 m a.s.l. and upstream of the Yesa Reservoircovers an area of 2191 km^2 with diverse lithology: i) magmatic and sedimentary Paleozoic rocks in the axial part: ii) calcareous Mesozoic rocks, and Tertiary sandstones and marls of the Eocene Flysch in the Internal Ranges; iii) Eocene marls covered by Quaternary glacis and terraces in the Internal Depression and iv) conglomerates and sandstones in the Eocene-Oligocene External Ranges.

The Flysch is the predominant formation covering as much as 55 % of the total surface. The main processes contributing to the supply of sediments and the siltation of the Yesa Reservoirare debris flows and slumps in the Axial and Internal Ranges (Lorente et al., 2002) and intensive gullying on the marls at the Internal Depression and water erosion with abundant rills in the Flysch Sector (Navas et al., 1997, 2005a).

The climate is transitional from temperate Atlantic to continental Mediterranean. Mean annual rainfall varies between around 1500 mm in the Internal Ranges and 800 mm in the Internal Depression. The distribution of natural vegetation follows an altitudinal pattern (Villar et al., 2001) from high mountain meadows, pine tree forest with some shrubs and the oak domain that was transformed into farmland in the last centuries.

In the reservoir the main environments are the delta area at the mouth of the river, the submerged plains and the dam wall delta (Navas et al., 2008). The sedimentary sequence established from cores that were retrieved from the submerged plains comprises the sediments accumulated during more than 41 years since the dam was in full operation until the coring campaign that were supplied mainly during floods (Navas et al., 2009). In this study based on detailed sedimentological information that was linked with data on the hydrological regime it was possible to distinguish three main periods of infilling. The first period extending from the reservoir construction until 1979 had the highest flood frequency of the reservoir history and was characterized by a succession of fining upward sequences deposited successively in each flood. The second period (1979–1988) also registered a high sedimentation rate as result of the most intense floods for the whole studied period. The third period (1988–2000) had lower sedimentation coinciding with lower discharges and less frequent floods.

2.2 Core sampling and analyses

The radiological and geochemical characteristics of sediments accumulated in the reservoir were studied in two sediment cores (Y1 and Y2) and one sediment profile (Y3) that were collected along the reservoir axis at the submerged central plains (Figure 1). This part of the reservoir is considered the most stable and suitable environment to obtain a representative record of the materials accumulated in the bottom of the reservoir (Valero-Garcés et al., 1999; Navas et al., 2004).

In site Y3 the sedimentary profile (400 cm) was sampled during a survey carried out when the water level at the reservoir was very low and the meandering channel of the Aragón River was exposed. A section from the base to the top of the profile was hand excavated and samples of fresh sediment were collected at different depth intervals. The cores Y1 and Y2 were retrieved using a hand operated, modified Livingstone corer. The length of the cores was 450 cm for core Y1 and 425 cm for core Y2. When the submerged plains were exposed it was estimated that the total thickness of the deposit at the core sites reached 5.5 to 6.5 m; however, this total depth was not attained in the cores.

The sediment sampling considered the differences in the sedimentary record associated to different floods. The changes in sediment composition and grain size that were previously identified based on analyses performed on alternate 1 cm samples served to discriminate sedimentological facies in the sequence (Navas et al., 2009). Thus, sampling intervals were established after consideration of such differences in order to ascribe the radiological and geochemical properties to specific layers corresponding to different events.

The cores were split in half by using a cutter and a thin metal wire. A total of 21 and 13 samples were selected in cores Y1 and Y2, respectively, and 18 samples in profile Y3. Samples were placed in plastic bags for storage and kept refrigerated for laboratory processing and analysis. They were air dried and weighted following standard procedures. In the samples of the selected intervals grain size, general composition, radionuclides and stable elements were analysed as well as mineralogy in profile Y3. The results represented in the figures correspond to the middle of the sampled interval.

Grain size analysis of different size fractions were done by using laser equipment after particles were stirred, chemically disaggregated and ultrasonically dispersed. The composition of sediments, organic matter and carbonate contents and the residual fraction (mostly silicates) were measured by loss on ignition. The analysis of the total elemental composition was carried out after total acid digestion with HF (48%) in a microwave oven. Samples were analysed for the following 17 elements: Li, K, Na (alkaline), Mg, Ca, Sr, Ba (light metals) and Cr, Cu, Mn, Fe, Al, Zn, Ni, Co, Cd and Pb (heavy metals). Analyses were performed by atomic emission spectrometry using an inductively coupled plasma ICP-OES (solid state detector). Concentrations, obtained after three measurements per element, are expressed in mg kg^{-1}.

In profile Y3 the mineralogical composition was determined by means of X-ray diffraction using a difractometer equiped with a Si-Li detector using Cu Kα radiation on random powder of bulk sample. The <2µ fraction was studied on oriented samples after standard treatments. The reflecting powers of Schultz (1964) for bulk sample were used for the quantitative estimation of the identified minerals.

Radionuclide activity in the samples was measured using a high resolution, low background, low energy, hyperpure coaxial gamma-ray detector coupled to an amplifier and multichannel analyser. The detector had a 20% efficiency, 1.86 keV resolution (shielded to reduce background) and was calibrated using standard samples that had the same geometry as the measured samples. Subsamples of 50 g were loaded into plastic containers. Count times over 24 h provided an analytical precision of about ± 5 to ± 15 % at the 95% level of confidence. Activities were expressed as Bq kg^{-1} dry soil.

Gamma emissions of ^{238}U, ^{226}Ra, ^{232}Th, ^{40}K, ^{210}Pb, and ^{137}Cs (in Bq kg^{-1} air-dry soil) were measured in the bulk sediment samples. ^{238}U was not analysed in profile Y3. Considering the appropriate corrections for laboratory background, ^{238}U was determined from the 63-keV line of ^{234}Th, the activity of ^{226}Ra was determined from the 352-keV line of ^{214}Pb; ^{210}Pb activity was determined from the 47 keV photopeak, ^{40}K from the 1461 keV photopeak; ^{232}Th was estimated using the 911-keV photopeak of ^{228}Ac, and ^{137}Cs activity was determined from the 661.6 keV photopeak.

3 Results and discussion

In the Yesa Reservoir, the sediments that have accumulated on the submerged plains are mostly silt (median range between 63 – 73 %), with much smaller proportions of clay (16 – 23 %) and sand (8 – 13 %) (Table 1). Although the Y1 core had comparatively less sand and the Y2 core had comparatively more clay, the distribution of grain sizes was quite similar in the sediments at the three sampling sites. The percentage of the sedimentological facies as assessed by grain size, colour and sediment composition indicated that sandy and silty layers were most abundant in the profile (Y3), where they represented 90 % of the total sedimentary record, whereas clayey and silty clay layers predominated in the cores with the highest percentage in Y2 core (82 %).

Silicates and carbonates were the main components of the sediments which had homogeneous vertical distributions, and the amounts of organic matter were small (median range = 2.8 - 4.0 %). In the profile, the median of the residual fraction, i.e. silicates, accounted for as much as 80%, and was, on average, 20% higher in the profile than it was in the two cores. Carbonates constituted ~40% of the cores, but only 18% of the profile. In the cores, the distribution of the silicate and carbonate components varied little with depth.

The differences between the profile, which indicated a predominance of silicates and the abundance of sandy layers, compared to the two cores, which revealed a substantial carbonate component and an abundance of the

finest fractions, might have resulted from the location of the profile, which was at the talweg of the river channel. That location favoured the entrance of sandy materials into the inner parts of the reservoir. In addition, the greater energetic relief and the inflow from gullies near the site of the profile might have contributed to the high abundance of coarse materials in the profile. The mineral composition of the profile, was calcite (39%), quartz (28%), clays (26%), plagioclase (4%), dolomite (2%), and feldspars (1%) (n=18 samples).

In the sediments of the cores and the profile, radioisotope activities were 20-43 Bq kg^{-1} for ^{238}U, 14-40 for ^{26}Ra, 7-56 Bq kg^{-1} for ^{210}Pb, 19-46 Bq kg^{-1} for ^{232}Th, 1-48 Bq kg^{-1} for ^{137}Cs, and 185-610 Bq kg^{-1} for ^{40}K. Those levels are similar to those found in the soils of the Flysch Formation in the Yesa Basin (Navas et al., 2005b) where ^{137}Cs accumulates in the top layers while natural radionuclides are more homogeneously distributed in the soil depth profile. In sandstones, the normal concentrations of uranium and thorium are 0.5–2.0 ppm and 1–7 ppm, respectively, and in limestones, uranium and thorium concentrations are ~2 ppm (Faure, 1986). In the Yesa Basin, sandstones and limestones are the most abundant lithologies. Typically, in sedimentary rocks that have homogeneous mineral compositions, such as the marls and sand materials in the main formations of the Yesa Basin, radionuclide concentrations are constant (Faure, 1986). Of the radionuclides detected in the Yesa Reservoir, ^{40}K had the highest activity levels. In the sediments that accumulated in an ancient Roman reservoir in southwestern Spain, ^{40}K also exhibited the highest activity (Baeza et al., 2009). Among the cores and the profile collected in the Yesa Reservoir, the vertical distributions of the artificial radionuclide ^{137}Cs and, to a less extent, ^{210}Pb and ^{40}K, were highly variable; the levels of ^{226}Ra and ^{232}Th were the less variable and had the most homogeneous vertical distributions. The radionuclide activities were within the range of the background levels of the natural gamma radionuclides in the soils of a Flysch catchment, which is the formation that covers the most area in the Yesa Basin (Navas et al., 2011). In addition, activity levels were within the ranges found in surface formations in North America (Litaor, 1995; de Jong et al., 1994) and Germany (Fujiyoshi & Sawamura, 2004), but were less than the levels of ^{238}U, ^{226}Ra, ^{232}Th, ^{40}K, and ^{210}Pb detected in the sediments of the ancient Roman Proserpina Reservoir in southwestern Spain (Baeza et al., 2009). Those high activity levels are attributed to the geological environment of the reservoir, which is within the Hesperic Spanish Massif, and consists of metamorphic rocks that have levels of radionuclides that are higher than those in the sedimentary rocks that predominate in the basin of the Yesa Reservoir.

In the two cores from the Yesa Reservoir, most of radionuclide activities were quite similar, but they differed from those found in the profile (Fig. 2). The levels of ^{226}Ra, ^{232}Th, ^{210}Pb, and ^{137}Cs were significantly higher in the profile than they were in the two cores, as indicated by an ANOVA (Table 2), probably, because of the high silicate content of the former and the inflow of mineral rich waters from Tiermas, a thermal source near the site where the profile was collected. With the exception of ^{210}Pb and ^{137}Cs, the lowest levels of radionuclides were in the Y1 core, which was located near the inflow from the Aragón River.

The high levels of ^{137}Cs might have been related to the supply of sediments from the gullies that reach the area near the site of the profile, which are likely to transport eroded soil that contains ^{137}Cs. Increasing mean values of ^{226}Ra were found following the submerged canal of the Aragón river. The two cores and the profile differed significantly in the levels of ^{226}Ra which was lowest at the site near where the Aragón River flows into the reservoir (core Y1) and highest in the profile (Table 2) because the profile has higher silicate contents than the cores.

The activity levels of ^{238}U in the Y2 core were significantly lower than the levels in the Y1 core. ^{238}U and ^{226}Ra, which belong to the uranium series, differ greatly in their solubility, which affects their mobility, and ^{238}U is mobilized in forms of uranyl complexes (MacKenzie, 2000). The activity levels of ^{40}K appeared to be directly associated with the mineralogy of the sediments. The level of ^{40}K was highest in the Y2 core, which likely resulted from the abundance of clayey layers and clay fractions in this core.

In the profile, the levels of the natural radionuclides were significantly positively correlated, which suggests that they had a common source (Table 3). In addition, the correlations between the radionuclides were stronger and more likely to be statistically significant in the profile than they were in the cores. The low correlation between ^{210}Pb and ^{226}Ra in the cores is due to disequilibrium between the radionuclides (Krishnaswami et al., 1975; Bacon et al., 1976) caused by differences in the processes of geochemical differentiation (Benninger et al., 1975; Fleischer, 1983). Preferential mobilization and scavenging by particulate material is also described for the removal of Pb-210 in the interphase water-sediment (Chi-Ju et al., 2004). This process is favoured in porous and fissured materials and depends on the particulate size (Mercer, 1976) which agrees with our results that also suggest that this disequilibrium preferentially occurs in sand and silt materials.

In the Y2 core, the only significant correlations were between ^{226}Ra, ^{40}K, and ^{232}Th. It is suggested that the sediments in the profile were mainly contributed from the surface soil containing high ^{137}Cs and silicate minerals with high natural radionuclides, while subsoils containing no ^{137}Cs and high carbonate minerals made considerable contributions to the sediments in the cores.

In the profile, the activities of ^{210}Pb, ^{226}Ra, ^{232}Th, and ^{40}K tended to be positively correlated with the contents of the finest grain size fractions but the opposite occurs with sand (Table 4). The strong positive correlation between the activities of ^{40}K and clay content reflects the tendency for this radionuclide to be associated with clay minerals because radioisotopes can adsorb to clay surfaces or become fixed within the lattice structure (e.g. Jasinska et al., 1982; Vanden Bygaart & Protz, 1995). In the two cores, however, the correlations among radionuclides and sediment components were not as strong and less likely to be statistically significant. In the Y1 core, the amounts of organic matter and silicate materials of the residual fraction were significantly positively correlated with the abundance of each of the radionuclides, but the opposite was true for the relationships between carbonate content and the levels of the radionuclides. By comparison, in the cores, particularly Y2, the correlations between the levels of the radionuclides and the amounts of organic matter, silicates, carbonates, and grain size fractions were weaker and less likely to be statistically significant. In the cores, the radionuclides transported with the sediments were more likely to be affected by changes in the hydrological regime than were those in the profile, which was from a site where changes in the supply of radionuclides can be masked by the local input of radionuclides from the thermal source of Tiermas.

3.1 Relationships between the radionuclides and stable elements

In the profile and the cores from the Yesa Reservoir (Table 5), Ca, Al and Fe, in that order, were the most abundant elements and K, Na and Mg were also present in significant amounts. Barium, Mn, Sr and Li were less common and the concentrations of the heavy metals Zn, Pb, Cr, Ni, Cu, Co and Cd were low. The concentrations of the major and trace elements were within the ranges found in the soils in the Yesa Basin (Navas and Machín, 2002) and those found in soils developed on similar parent materials (Kabata-Pendias and Pendias 2001).

In the profile, the Na content was higher and Ca content was lower than in the cores; however, contents of Pb in the cores were nearly three times higher than the content in the profile. Typically, Pb is associated with clay minerals (Norrish 1975). The content of Zn was higher in the Y2 core than it was in the profile and the Y1 core. Similarly to Pb, Zn is generally associated with clay minerals, and the highest abundance of the clay fraction was found in the Y2 core. The contents of Ba and Mn and, to a lesser extent, Sr, were high in the Y2 core. Typically, Ba, Mn, and Sr are associated with feldspars (Kabata-Pendias and Pendias (2001), which likely are contained in the most abundant clay size fraction in the Y2 core. Thus, the elements that are associated with clay and feldspars minerals and were most abundant in the cores, appeared to be associated with the abundance of clayey layers in the cores.

The cores and the profile differed most significantly in the amounts of trace elements. The contents of Cr, Ni, Cu, and Co in the profile were ten times higher than the contents in the cores, and Cd occurred in the profile, only. The high content of microelements in the profile likely was related to the thermal source of Tiermas that may supply substantial amounts of Cr, Ni, Cu, Co and, to lesser extent, Cd that came from the mineral rich waters. In addition, the abundance of silicates in the sediment composition of the profile may also contribute to the high contents of radionuclides and trace elements because heavy metals and radionuclides are enhanced in argillaceous materials (Kabata-Pendias and Pendias 2001).

In the profile, among the direct and significant correlations those between ^{226}Ra, ^{232}Th, ^{210}Pb, ^{40}K, with K and Mn, and between ^{226}Ra, ^{232}Th and ^{40}K with Cu and Cd (Table 6), suggests that these radionuclides and the stable elements were from a common source. However, the activities of fallout ^{137}Cs were not correlated with the stable element contents, which confirmed that this artificial radionuclide had a different source. In the Y1 core, some of the relationships between the radionuclides and the elements differed from those detected in the profile. The activities of most of the radionuclides were inversely correlated with the contents of Ca and Sr, which suggested the absence of a link with carbonates. Although the radionuclide activities were positively correlated with contents of Zn, Cr, and Fe, the reverse was true in the profile. In the Y2 core, the relationships between radionuclides and stable elements were much less clear and only a few correlations were statistically significant.

3.2 Vertical distribution of the ^{238}U/^{226}Ra and ^{232}Th/ ^{226}Ra activity ratios

The uranium and thorium series are commonly associated in nature. Ivanovich (1994) reported a quasi-constant mass ratio of those decay series in natural systems, although this equilibrium is often disturbed by physical and chemical processes that enhance a loss or gain of a given decay product. Thus, activity ratios between parent/parent or between progeny pairs can be used to assess the maintenance of the initial proportionality between the ^{232}Th and ^{238}U decay series. Furthermore, ^{238}U/^{226}Ra activity ratios can be used to ascertain equilibrium within the same decay series. If secular equilibrium prevails in the ^{238}U chain, the activity ratios of ^{238}U/ ^{226}Ra will be approximately 1; therefore, values other than 1 indicate disequilibrium. In the sedimentary record of the Yesa Reservoir, most of the samples in the cores had ^{238}U/^{226}Ra ratios that were >1.0, which indicated disequilibrium in the ^{238}U chain (Table 7). Ratios higher than 1 suggest ^{238}U enrichment which might have been due to large differences in the mobility of these radionuclides (e.g., Dowdall and O'Dea, 2002). Disequilibrium was greater in the Y1 core than it was in the Y2 core, and the greatest deviations from the linear trend occurred in the upper 200 cm of both cores, where sediments of fine grain size were most abundant. In addition, sorption is an important component of the U cycle (Kabata-Pendias and Pendias, 2001) and significant

accumulations of U are often associated with clays because the clay fraction has an affinity for absorbing U and Th (Megumi et al. 1982).

The ^{232}Th/ ^{226}Ra activity ratio (i.e., the progeny pair ^{228}Ac/^{214}Pb) can be used to assess the maintenance of the proportionality within the ^{232}Th and ^{238}U decay series, which is about 1.1 in most environmental samples (Evans et al. 1997). In our study, most of the samples had ^{232}Th/ ^{226}Ra activity ratios that were >1.1, although the deviations from the original proportionality were less than they were for the ^{238}U / ^{226}Ra ratio. In the profile, deviations from the linear trend were highest in the first 200 cm, but this was not observed in the cores, where the ^{232}Th/ ^{226}Ra activity ratio remained constant throughout the depth of the sedimentary record. Like ^{238}U, ^{232}Th can be easily mobilized in forms of organic compounds and various complex inorganic cations that can be absorbed by clays, which contributes to the differential mobility of ^{232}Th and ^{226}Ra.

3.3 The vertical distribution of radionuclides in the reservoir sediments

Variations in radionuclide activities with depth in the sedimentary sequence of the Yesa Reservoir might provide insights into the patterns and pathways of the terrestrial radioactivity (Fig. 3). In the profile, the activity levels were constant with depth, with the exception of a tendency for ^{137}Cs to be more prevalent and ^{232}Th to be more highly dispersed in the upper 200 cm of the profile. In the Y1 core, with the exception of ^{137}Cs, the levels of the radionuclides decreased slightly with depth, which appeared to be related to the predominance of sandy materials at the lower portion of the core. Similar to the profile, in the Y1 core, the activities of ^{226}Ra and ^{232}Th were the most constant during the infilling period, while the activities of ^{137}Cs varied the most and were highest in the deepest layers, which reflects temporal changes in its global fallout. The activities of ^{238}U were higher in the upper 200 cm than they were in the lower portion of the core. In the Y2 core, the pattern was not as clear because positive (^{226}Ra, ^{232}Th, ^{40}K) and negative (^{210}Pb, ^{137}Cs, ^{238}U) trends were apparent, which reflected increases and decreases in activity levels, respectively, with depth. In the Y2 core, with the exception of ^{210}Pb and ^{137}Cs, whose activities varied widely with depth, the radionuclides were distributed homogeneously, which indicated that their supply was constant throughout the infilling period, but this is also associated with low variation in the composition and the distribution of grain sizes in the sedimentary layers.

In general, for the entire sedimentary record in the reservoir, the more stable activities of ^{226}Ra and ^{232}Th reflect the almost constant contributions throughout the infilling period. The activities of ^{40}K and ^{210}Pb were more variable, but the greatest variation was in ^{137}Cs, which was a consequence of the pattern of its fallout, globally, and the close association between ^{137}Cs and the fine soil particles that are mobilized by physical processes such as erosion. The timing of starting operation of the reservoir was almost coincidental with the onset of ^{137}Cs fallout whose content has decreased with time (^{137}Cs half life is 30.17 yr) since its fallout started until early eighties when its fallout ceased (Chernobyl ^{137}Cs fallout in the area was negligible). However, sediment age is unlikely to exert an important control on the activity levels of ^{137}Cs by comparing with the intense sedimentary dynamic that deposited more than 6 m of sediments at the submerged plains of the reservoir.

In general, the activity levels of the radionuclides were lowest in the layers of the sediment that had predominantly coarse fractions; i.e., sandy layers had the least radionuclide content (Figs. 4, 5, 6). The activity levels of the radionuclides were highest in the layers that were composed of clayey materials. In the Y1 core, collected near the point where the Aragón River flows into the reservoir, radionuclide content was lowest at the bottom of the core in a thick layer of coarse grey sands, which indicated the occurrence of an extreme flood, and

in a sandy layer 32.5 cm from the top of the core, which was deposited by another intense flood. The infilling of the Yesa Reservoir occurred as a succession of fining upwards sequences, each reflecting major floods episodes that have characteristic patterns of the frequency and intensity of floods which appear to be correlated with the activity levels of the radionuclides.

Features of the sedimentary record, such as the distribution of fining up grain size sequences, the thickness and distribution of alternating layers, helped to identify the three deposition units that occurred during the period of infilling (Navas et al., 2009). Frequent, regular periods of floods in the period 1959-1979 were accompanied by the regular deposition of up-fining sequences. In the period 1979-1988, there were fewer floods. In the period 1988-2000, floods were less intense, but occurred more frequently than they did in the previous period, which was paralleled by less energetic silty fining upward sequences. Consequently, radionuclide activity levels in the sandy layers that marked the beginning of a flood were low. The levels of ^{137}Cs were highest in the lower section of the Y1 core (depth = 336-392 cm) and were associated with clayey layers. In a reservoir on the Loess Plateau, China, ^{137}Cs concentrations were highest in the finest sediments of the infilling sequences caused by floods (Zhang et al., 2006). The radioisotopes ^{137}Cs and unsupported ^{210}Pb can be used to discriminate sources of reservoir sediments (e.g., Foster et al., 2007, Simms et al., 2008).

In the Yesa Reservoir, sandy material was most abundant (almost 25%) in the core (Y1) that was collected near the entrance of the Aragón River. Clayey and silty clay layers were more predominant (82%) in the Y2 core than in the Y1 core (40%) which is the main reason why the variations in radionuclide activity levels were not as marked in the former as they were in the latter. The more marked pattern in the variation of the radionuclides in the profile resulted from the high frequency of alternations between sandy and clayey layers. The highest activity levels of all of the natural radionuclides occurred at depths of 200 cm, 255 cm, and 365 cm, which coincided with the period of the highest frequency of intense floods occurring in the lower part of the profile and the predominance of less frequent and less energetic floods in the upper part of the sedimentary record. In addition, the highest levels of ^{137}Cs occurred in the profile between 200 cm and 225 cm, which coincided with periods of frequent, high-intensity floods, which would have triggered intense erosion in the Yesa Basin. In general, ^{137}Cs content decreased at the upper part of the cores and the profile. ^{137}Cs remains strongly fixed to the fine soil fractions and has little mobility; thus, it would have been transported with eroded materials. In a reservoir on the Danube River which had a predominance of silty sediments, ^{137}Cs was concentrated in < 20 μm fractions of organic material, clays and Fe and Mn oxides, the radionuclides varied little and activity levels also increased with decreasing grain size (Rank et al., 1987).

In the profile, all of the radionuclides showed quite parallel depth distributions, although ^{226}Ra and ^{232}Th, the least mobile of the radioisotopes, did not exhibit marked peaks in activity. The depths at which the maximum levels of radioisotope activity occurred were similar in the Y1 core and the profile, which suggests that the transport of the radionuclides through the reservoir occurred during the same floods and that the distribution of radionuclides was the same near the entrance as it was in the inner section of the reservoir. Furthermore, the local input of radionuclides identified in the profile, which were associated with the thermal sources at Tiermas add to the content of radionuclides transported with the sediments.

Differences in the frequency, intensity, and occurrence of floods and the variations in the hydrological regime led to differences in the characteristics of the sediments. Furthermore, those differences appear to have affected the distribution of radionuclides. The activity levels of the natural radionuclides were highest at the

lower part of the sedimentary record, which coincides with an energetic fluvial regime that caused the highest sedimentation rates in the reservoir (Navas et al., 2009).

4 Conclusions

In the last half-century, the infilling of the Yesa Reservoir, Spain, produced variable sedimentological characteristics that were attributed to variations in the hydrological regime of the Aragón River and its tributaries that drained the catchment, which, in turn, has affected the distribution of radionuclides within the sedimentary sequence.

In the Yesa Reservoir, the sediments which arrive mainly during floods and, subsequently, are redistributed in ways that are influenced by the water level in the reservoir, had radionuclide levels that are within the range observed in similar environments. Variation in radionuclide activities is associated with the grain size and composition of the accumulated sediments. Enriched activity levels are associated with clayey and silty layers, and depleted levels are associated with sandy layers that have predominantly coarse fractions. Clearly, sedimentological processes influence the patterns of radionuclide accumulation. The distributions of the radionuclides were consistent with the history of the infilling of the reservoir and with the processes of transport and the accumulation of sediments.

The levels of radionuclides and stable elements were higher in silicate-rich sediments such as those in the profile compared to those in the cores. Enhanced levels of radionuclides and some stable elements were associated with the mineral-rich thermal source of Tiermas, which is near the site where the profile was collected.

The sedimentary record in the Yesa Reservoir provided an opportunity to quantify the abundance and distribution of radionuclides, which is of importance to compare with environmental baselines in order to preserve the quality of water bodies. The methods used in this study delivered information that permitted an assessment of the patterns of accumulation of radionuclides in reservoir sediments and allowed the identification of natural inputs into the system and its differentiation from the fluvial transport and reservoir deposition.

Assessments of the radionuclides that are contained in the sedimentary records of reservoirs can provide insights into the processes that are involved in the mobilization of radionuclides in terrestrial ecosystems and help to understand the pathway by which radionuclides are mobilized in the environment.

Acknowledgements Financial support from CICYT project MEDEROCAR (CGL2008-00831/BTE) is gratefully acknowledged.

References

Bacon MP, Spencer DW, Brewer, PG (1976) ^{210}Pb /^{226}Ra and ^{210}Po ^{210}Pb disequilibria in seawater and suspended particulate matter. Earth Planet Sc Lett 32:277-296.

Baeza A, Guillén J, Ontalba Salamanca, MA, Rodrıíguez A, Ager FJ (2009) Radiological and multi-element analysis of sediments from the Proserpina reservoir (Spain) dating from Roman times. J Environ Radioactiv 100:866–874.

Benninger LK, Lewis DM, Turekian KK (1975) On the use of natural Pb-210 as a heavy metal tracer in the river—Estuarine system. In: Marine Chemistry in the Coastal Environment. ACS Symposium Series, Vol. 18, Chapter 12, pp 202–210.

Callender E, Robbins JA (1993) Transport and accumulation of Radionuclides and Stable Elements in a Missouri River Reservoir. Water Resour Res 29(6):1787-1804.

Chi-Ju L, Yu-Chia C, Tsung-En W (2004) Ra-226 and Pb-210/Ra-226 Activity Ratio in the Northern South China Sea. In: American Geophysical Union, Spring Meeting 2004, abstract #OS41A-0.

de Jong E, Acton DF, Kozak LM (1994) Naturally occurring gamma-emitting isotopes, radon release and properties of parent materials of Saskatchewan soils. Can J Soil Sci 74:47-53.

Dowdall M, O'Dea J (2002) Ra-226/U-238 disequilibrium in an upland organic soil exhibiting elevated natural radioactivity. J Environ Radioactiv 59 (1):91-104.

Evans CV, Morton LS, Harbottle G (1997) Pedologic assessment of radionuclide distributions: use of a radio-pedogenic index. Soil Sci Soc Am J 61:1440-1449.

Faure G (1986) Principles of isotope Geology, 2nd Edition. Wiley. New York.

Fleischer, RL (1983) Theory of alpha recoil effects on radon release and isotopic disequilibrium. Geochim. Cosmochim. Acta 47(4):779–784.

Foster, IDL (2006). Lakes and reservoirs in the sediment delivery system: reconstructing sediment yields. In: Owens PN, Collins AJ (eds) Soil Erosion and Sediment Redistribution in River Catchments. CAB International, Wallingford, pp. 128–142.

Foster IDL, Boardman J, Keay-Bright J (2007) Sediment tracing and environmental history for two small catchments, Karoo Uplands, South Africa. Geomorphology 90:126–143.

Fujiyoshi R, Sawamura S (2004) Mesoscale variability of vertical profiles of environmental radionuclides (^{40}K, ^{226}Ra, ^{210}Pb and ^{137}Cs) in temperate forest soils in Germany. Sci Total Environ 320:177-188.

Ivanovich M (1994) Uranium series disequilibrium: Concepts and applications. Radiochim Acta 64:81-94.

Jasinska M, Niewiadomski T, Schwbenthan J (1982) Correlation between soil parameters and natural radioactivity. In: Vohra K, Mishra UC, Pillai, KC, Sadasivan S (eds) Natural radiation environment. John Wiley and Sons, New York. pp 206-211

Jordan C, Cruickshank JG, Higgins AJ, Hamill KP (1997) The soil geochemical atlas of Northern Ireland. Department of Agriculture for Northern Ireland. Belfast. UK.

Kabata-Pendias A, Pendias H (2001) Trace elements in soils and plants. 3rd ed. CRC. p. 413. Boca Raton, Fla.

Krishnaswami, S, Somayajulu, BLK, Chung, Y (1975) ^{210}Pb/^{226}Ra disequilibrium in the Santa Barbara basin. Earth Planet Sc Lett 27:388-392.

Litaor MI (1995) Uranium isotopes distribution in soils at the Rocky Flats Plant, Colorado. J Environ Qual 24:314-323.

Lorente A, García-Ruíz JM, Beguería S, Arnaez JM (2002) Factors explaining the spatial distribution of hillslope debris flows. A case study in the Flysch Sector of the Central Spanish Pyrenees. Mt Res Dev 22(1):32-39.

MacKenzie AB (2000) Environmental radioactivity: experience from the 20th century—trends and issues for the 21st century. Sci Total Environ 249:313–29.

McCall PL, Robbins JA, Matisoff G (1984) ^{137}Cs and ^{210}Pb transport and geochronologies in urbanized reservoirs with rapidly increasing sedimentation rates. Chem Geol 44:33-65

McLean RI, Summers JK, Olsen CR, Domotor SL, Larsen IL, Wilson H (1991) Sediment accumulation rates in Conowingo reservoir as determined by Man-Made and natural radionuclides. Estuaries 14(2):148-156.

Megumi K, Oka T, Yaskawa K, Sakanoue M (1982) Contents of natural radioactive nuclides in relation to their surface area. J Geophys Res 87:10857-10860.

Mercer, TT (1976) The effect of particle size on the escape of recoiling RaB atoms from particulate surfaces. Health Phys. 31:173–175.

Morellón M, Valero Garcés B, Moreno A, González Sampériz P, Mata P, Romero O, Maestro M, Navas A (2008) Holocene Paleohydrology and climate variability in Noertheastern Spain: The sedimentary record of lake Estanya (Pre-Pyrenean Range). Quatern Int 118:15-31.

Navas A, Machín J (2002) Spatial distribution of heavy metals and arsenic in soils of Aragón (NE Spain): controlling factors and environmental implications. Appl Geochem 17:961-973.

Navas A, Machín J, Soto J (2005a) Assessing soil erosion in a Pyrenean mountain catchment using GIS and fallout ^{137} Cs. Agr Ecosyst Environ 105:493-506.

Navas A, Soto J, Machín J (2005b) Mobility of natural radionuclides and selected major and trace elements along a soil toposequence in the central Spanish Pyrenees. Soil Sci 170:743-757.

Navas A, Valero-Garcés BL, Machín J (2004) An approach to integrated assessement of reservoir siltation: the Joaquín Costa reservoir as case study. Hydrol Earth Syst Sci 8 (6):1193-1199.

Navas A, Gaspar L, López-Vicente M, Machín J (2011) Spatial distribution of natural and artificial radionuclides at the catchment scale (South Central Pyrenees) Radiat Meas 46 (2):261-269.

Navas A, Valero-Garcés BL, Gaspar L, Machín J (2009) Reconstructing the history of sediment accumulation in the Yesa reservoir: an approach for management of mountain reservoirs. Lake Reserv Manage, 25 (1):15-27.

Navas A, García-Ruiz JM, Machín J, Lasanta T, Walling D, Quine T, Valero B (1997) Aspects of soil erosion in dry farming land in two changing environments of the central Ebro valley, Spain. In: Walling DE, Probst JL (eds) Human Impact on Erosion and Sedimentation IAHS Publi. 245:13-20.

Navas A, Valero-Garcés B, Gaspar L, García-Ruiz JM, Beguería S, Machín J, López-Vicente M (2008) Variabilidad espacial del transporte de sedimento en la cuenca superior del rio Aragón. Cuadernos de Investigación Geográfica, 34:39-60.

Norrisk K (1975) The geochemistry and mineralogy of trace elements. In: Trace Elements in Soil Plant-Animal Systems. Nicholas DJD, Egan AR (eds) Academic Press, New York, 55 pp.

Rank D, Kralik M, Gyurits KA, Maringer F, Rajner V, Kurcz I (1987) Investigation of sediment transport in the Austrian part of the Danube using environmental isotopes. IAEA-SM. 299(7):637-646.

Simms AD, Woodroffe C, Jones BG, Heijnis H, Mann RA, Harrison J (2008) Use of ^{210}Pb and ^{137}Cs to simultaneously constrain ages and sources of post-dam sediments in the Cordeaux reservoir, Sydney, Australia. J Environ Radioactiv 99:1111-1120.

Schultz LG (1964) Quantitative interpretation of mineralogical composition from X-ray and chemical data of the Pierre Shale. US Geol Surv Prof Paper. 391C.

Sundborg A, Rapp A (1986) Erosion and sedimentation by water: problems and prospects. Ambio 15:215-225.

Valero-Garcés BL, Navas A, Machín J, Walling D (1999) Sediment sources and siltation in mountain reservoirs: a case study from the Central Spanish Pyrenees. Geomorphology 28:23-41.

Valero-Garcés B, Moreno A, Navas A, Mata P, Machín J, Delgado-Huertas A. González-Sampériz P, Schwalb A, Morellón M, Edwards L (2008) The Taravilla lake and Tufa deposits (Central Iberian Range, Spain) as paleohydrological and paleoclimatic indicators Paleogeogr Palaeocl 259:136-156.

Vanden Bygaart AJ, Protz R (1995) Gamma radioactivity on a chronosequence, Pinery Provincial Park, Ontario. Can J Soil Sci 75:73-84.

Villar L, Sesé JA, Fernández JV (2001) Atlas de la Flora del Pirineo aragonés. II, Instituto de Estudios Altoaragoneses y Consejo de Protección de la Naturaleza de Aragón, Huesca y Zaragoza, p 790.

Walling DE, Owens PN, Foster IDL, JA (2003) Changes in the sediment dynamics of the Ouse and Tweed basins in the UK, over the last 100-150 years. Hydrol Proc 17:3245-3269.

Zhang X, Walling DE, Yang Q, He X, Wen Z, Qi Y, Feng M (2006) 137Cs budget during the period of 1960s in a small drainage basin on the Loess Plateau of China. J Environ Radioactiv 86:78-91.

FIGURES

Fig. 1 The Yesa Reservoir: location of cores (Y1, Y2) and the profile (Y3) retrieved along the river axis. Lithological and geo-structural units and landscape of the basin of the Yesa Reservoir, Aragón, Spain

Fig. 2 Box plots of the radionuclide activity levels in the sediments of the Yesa Reservoir, Aragón, Spain, corresponding to cores Y1, Y2, and profile Y3

Fig. 3 Variation trends of radionuclide activities with depth in the cores Y1, Y2, and profile Y3 of the Yesa Reservoir, Aragón, Spain

Fig. 4 Vertical distribution of the radionuclides (Bq kg^{-1}) in the sedimentological facies identified in core Y1 taken in the submerged plains of the Yesa Reservoir, Aragón, Spain

Fig. 5 Vertical distribution of the radionuclides (Bq kg^{-1}) in the sedimentological facies identified in core Y2 taken in the submerged plains of the Yesa Reservoir, Aragón, Spain

Fig. 6 Vertical distribution of the radionuclides (Bq kg^{-1}) in the sedimentological facies identified in the profile collected from the submerged plains within the Yesa Reservoir, near the village of Tiermas, Spain

Fig. 1

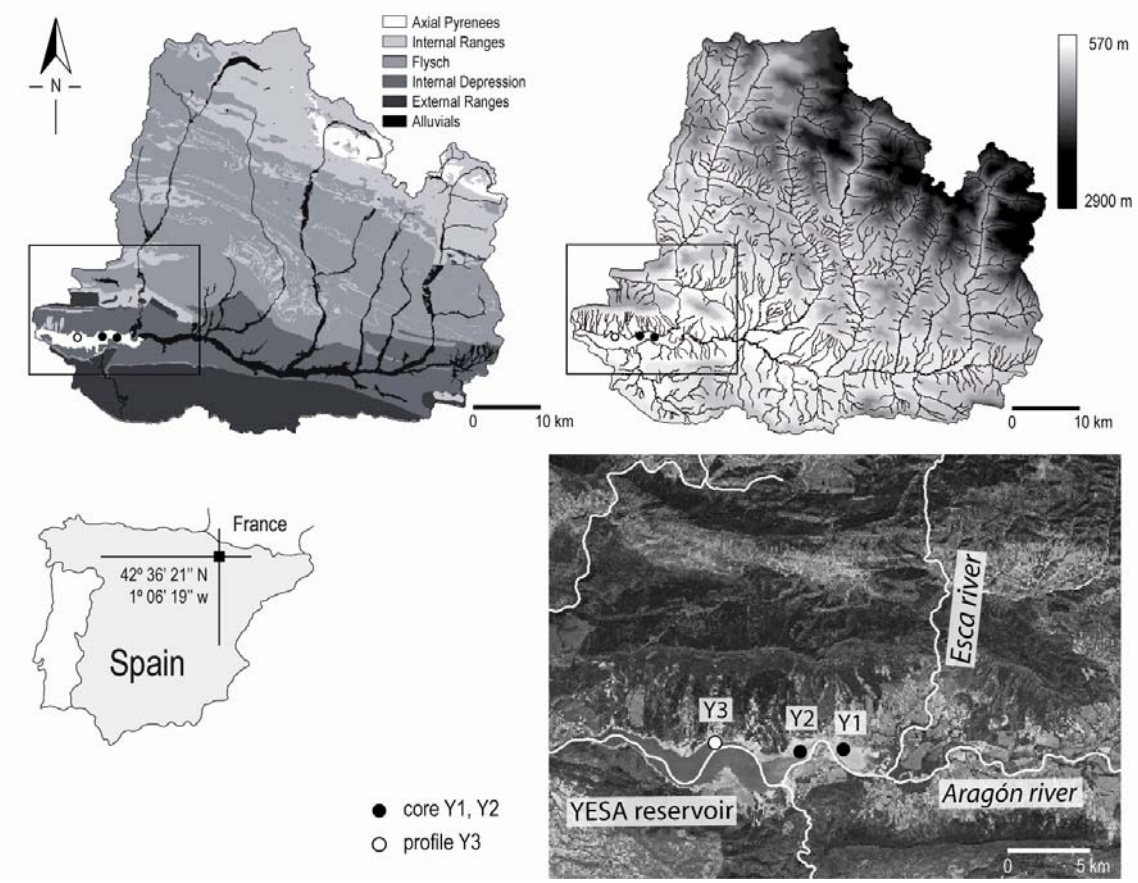
N
Axial Pyrenees
Internal Ranges
Flysch
Internal Depression
External Ranges
Alluvials
0
10 km
570 m
2900 m
0
10 km
France
42º 36' 21" N
1º 06' 19" w
Spain
core Y1, Y2
profile Y3
Esca river
Y3
Y2
Y1
YESA reservoir
Aragón river
0
5 km

Fig. 2

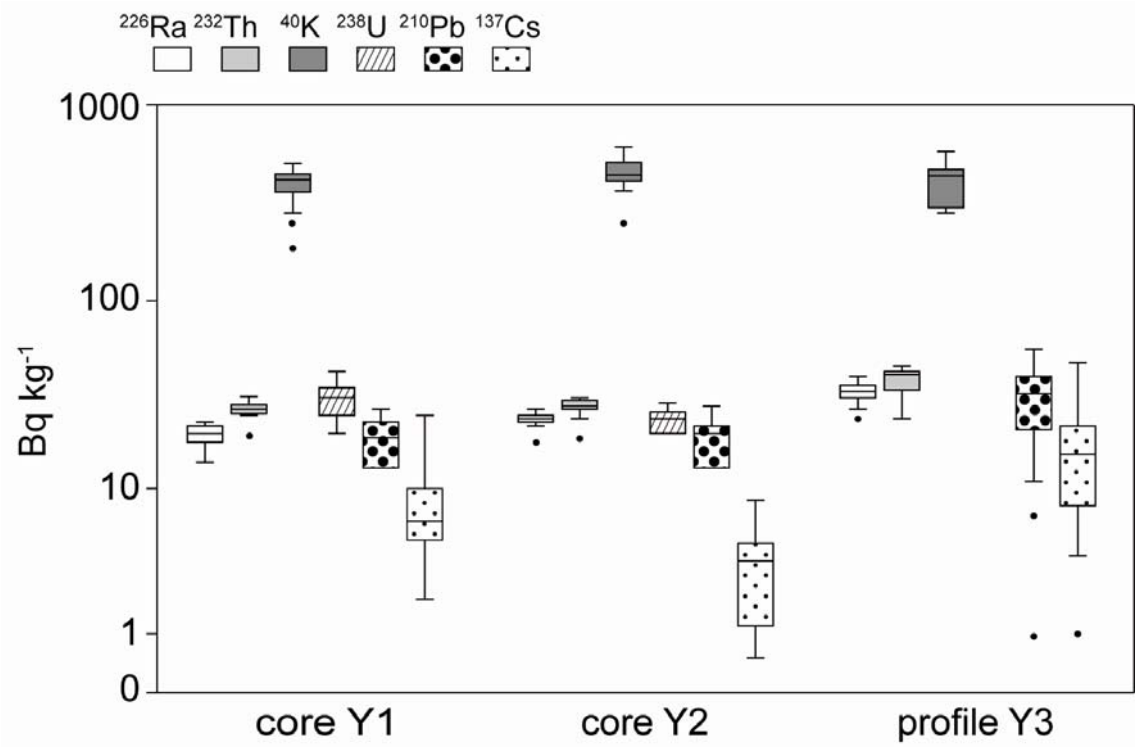
226Ra 232Th 40K 238U 210Pb 137Cs
1000
100
10
1
0
Bq kg-1
core Y1
core Y2
profile Y3

Fig. 3

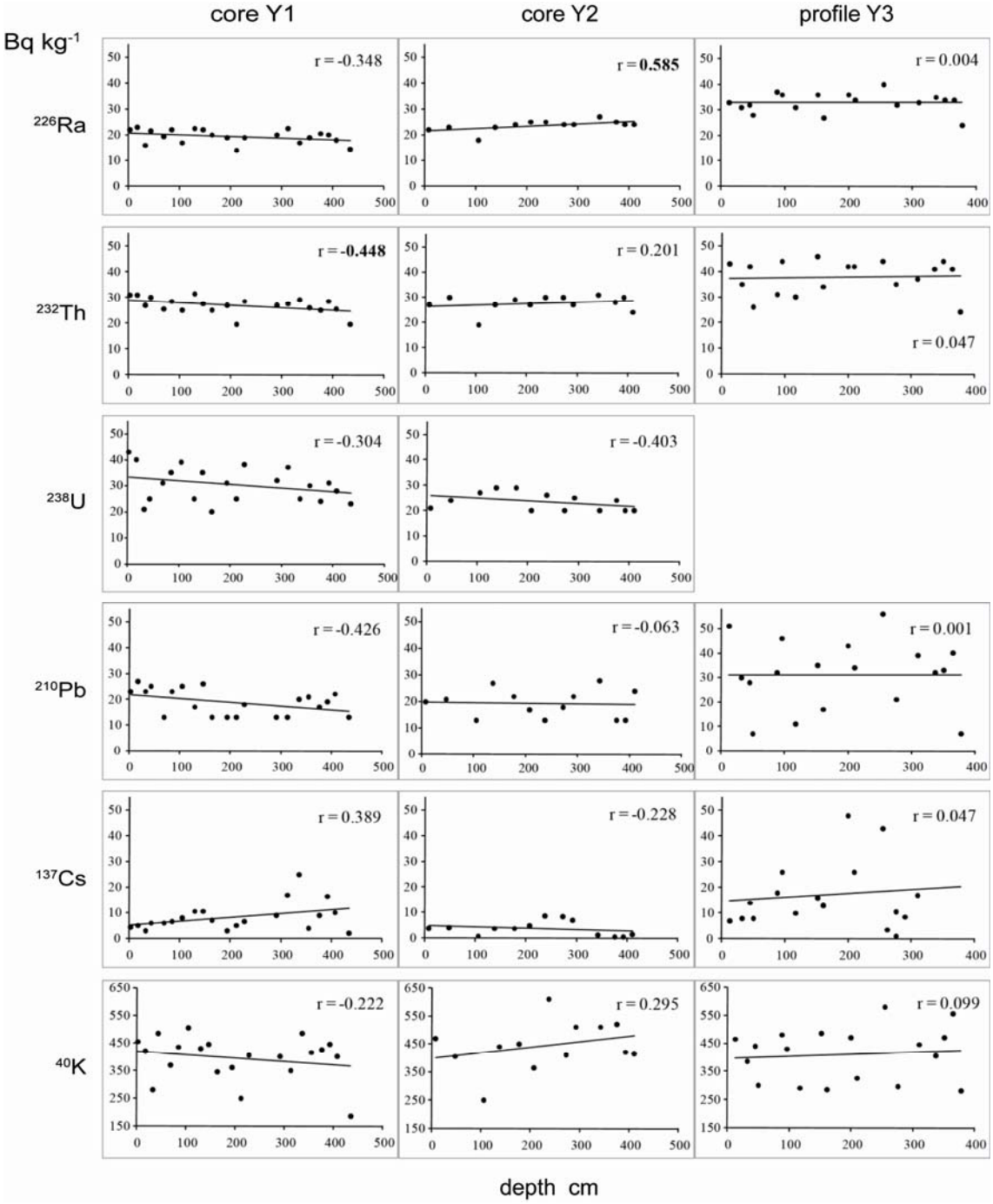
core Y1
core Y2
profile Y3
Bq kg-1
226Ra
232Th
238U
210Pb
137Cs
40K
r = -0.348
r = 0.585
r = 0.004
r = -0.448
r = 0.201
r = 0.047
r = -0.304
r = -0.403
r = -0.426
r = -0.063
r = 0.001
r = 0.389
r = -0.228
r = 0.047
r = -0.222
r = 0.295
r = 0.099
depth cm

Fig. 4

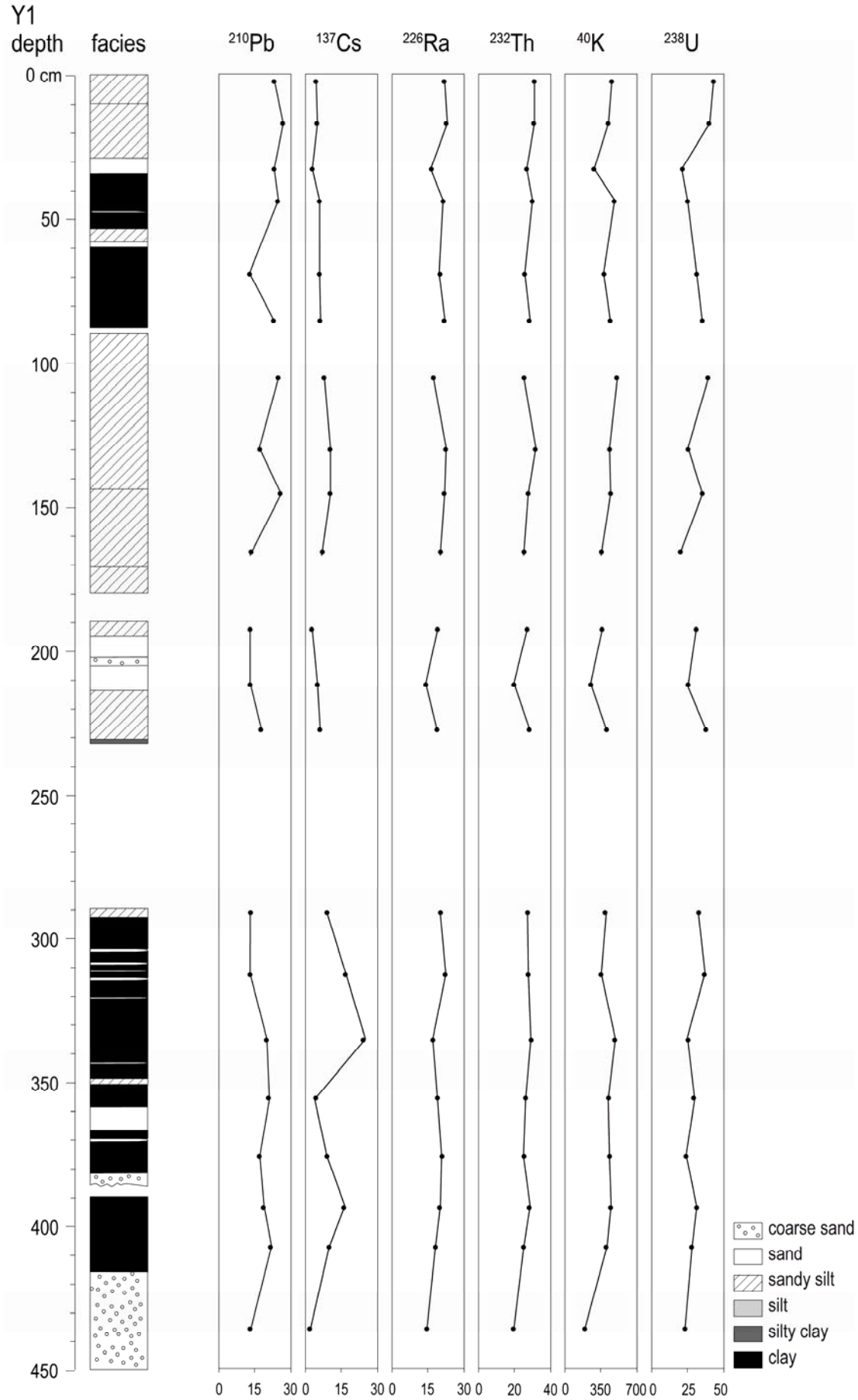
Y1
depth
facies
^{210}Pb
^{137}Cs
^{226}Ra
^{232}Th
^{40}K
^{238}U
0 cm
50
100
150
200
250
300
350
400
450
0 15 30
0 15 30
0 15 30
0 20 40
0 350 700
0 25 50
coarse sand
sand
sandy silt
silt
silty clay
clay

Fig. 5

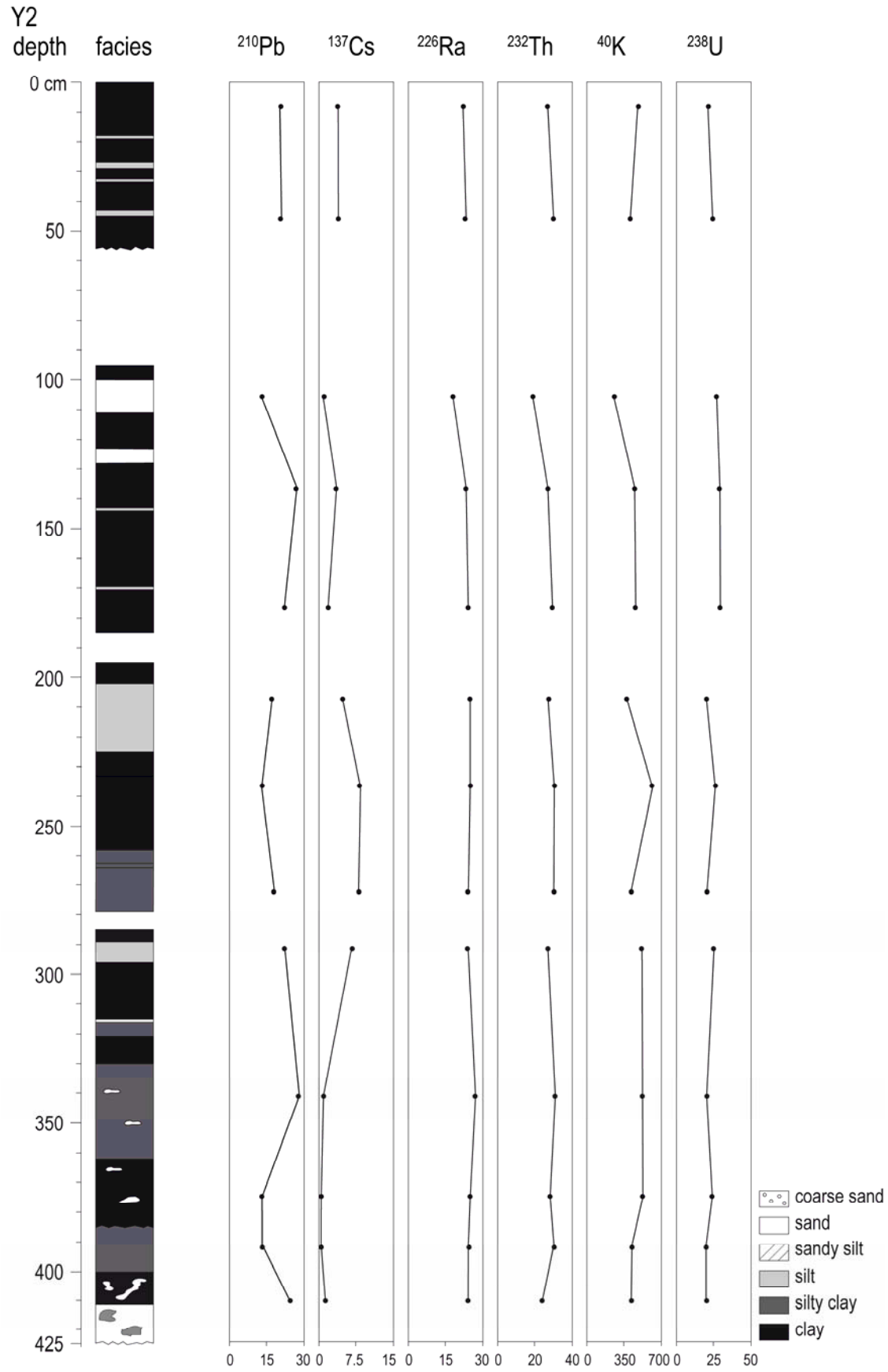
Y2
depth
facies
^{210}Pb
^{137}Cs
^{226}Ra
^{232}Th
^{40}K
^{238}U
0 cm
50
100
150
200
250
300
350
400
425
0 15 30
0 7.5 15
0 15 30
0 20 40
0 350 700
0 25 50
coarse sand
sand
sandy silt
silt
silty clay
clay

Fig. 6

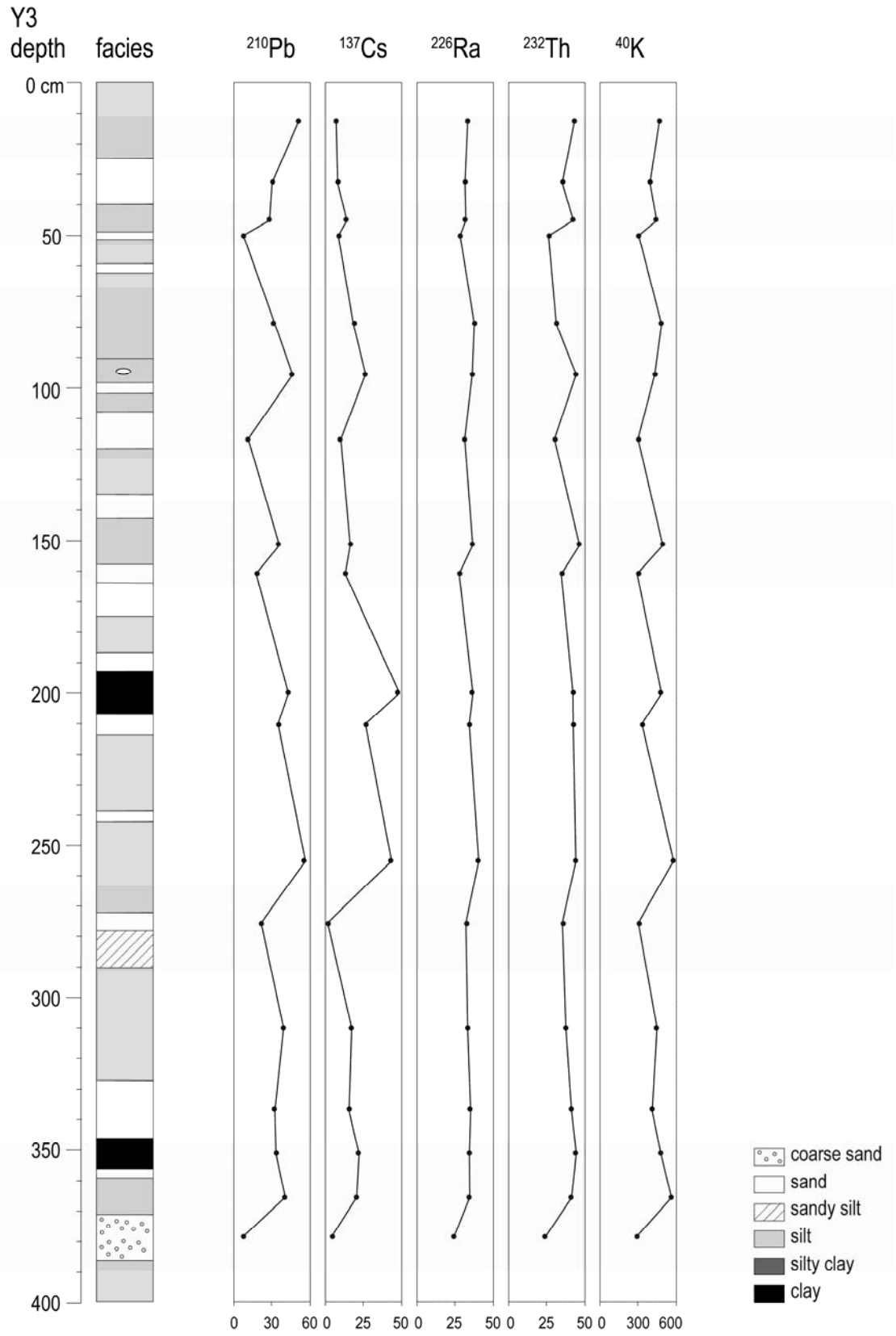
Y3
depth
facies
^{210}Pb
^{137}Cs
^{226}Ra
^{232}Th
^{40}K
0 cm
50
100
150
200
250
300
350
400
0 30 60
0 25 50
0 25 50
0 25 50
0 300 600
coarse sand
sand
sandy silt
silt
silty clay
clay

Table 1. Basic statistics of the distribution of the grain size fractions, organic matter and the general composition of the sediments accumulated in the bottom of the Yesa reservoir

		clay	silt	sand	OM	$CO_3^=$	residual
				%			
core Y1	n = 21						
	mean	17.9	67.3	14.8	3.7	42.0	54.4
	sd	4.8	12.9	16.5	0.9	8.4	8.3
	min	9.0	28.0	2.0	2.0	23.0	34.0
	max	29.0	77.0	63.0	5.0	64.0	75.0
core Y2	n = 13						
	mean	21.2	57.4	21.4	3.3	38.5	58.2
	sd	6.6	14.4	20.1	0.8	4.3	4.1
	min	8.0	20.0	6.0	2.0	30.0	51.0
	max	31.0	70.0	72.0	4.0	45.0	66.0
profile Y3	n = 18						
	mean	16.1	66.7	17.2	2.8	17.7	79.5
	sd	5.8	10.1	15.2	0.4	0.9	0.6
	min	9.1	47.7	0.4	2.0	16.2	78.6
	max	26.7	77.6	43.2	3.5	19.2	80.7

sd : standard deviation

Table 2. Basic statistics of the activity levels for the radionuclides assayed in the cores Y1, Y2 and profile Y3 retrieved from the sediments accumulated in the submerged plains of the Yesa reservoir.

		^{210}Pb		^{226}Ra		^{137}Cs		^{40}K		^{232}Th		^{238}U	
		Bq kg^{-1}											
core Y1	n=21												
	mean	18.9	a	19.5	a	8.3	a	394.8	a	26.9	a	30.4	a
	sd	5.0		2.6		5.5		79.5		3.2		6.7	
	CV %	26.7		13.5		66.4		20.2		11.8		21.9	
core Y2	n=13												
	mean	19.3	a	23.7	b	3.7	a	444.2	a	27.6	a	23.5	b
	sd	5.3		2.1		2.8		87.0		3.2		3.5	
	CV %	27.6		8.9		76.2		19.6		11.7		15.0	
profile Y3	n=18												
	mean	31.2	b	32.9	c	17.6	b	410.3	a	37.8	b	nd	
	sd	14.2		3.8		12.4		95.0		6.6		nd	
	CV %	45.5		11.7		70.4		23.1		17.6		nd	

sd: standard deviation.

nd: no data.

Different letters indicate significant differences at the 95% confidence level

Table 3. Pearson correlation coefficients between the radionuclide activities (Bq kg^{-1}) in the sediments of the Yesa Reservoir assayed in the cores Y1, Y2 and profile Y3.

core Y1

	^{210}Pb	^{226}Ra	^{137}Cs	^{40}K	^{232}Th
^{226}Ra	0.283				
^{137}Cs	-0.012	0.149			
^{40}K	**0.589**	**0.572**	0.427		
^{232}Th	**0.500**	**0.769**	0.284	**0.710**	
^{238}U	0.365	**0.463**	-0.005	**0.444**	0.420

core Y2

	^{210}Pb	^{226}Ra	^{137}Cs	^{40}K	^{232}Th
^{226}Ra	0.285				
^{137}Cs	-0.026	0.161			
^{40}K	0.113	**0.693**	0.356		
^{232}Th	0.162	**0.781**	0.325	**0.652**	
^{238}U	0.032	-0.374	0.111	0.041	-0.232

profile Y3

	^{210}Pb	^{226}Ra	^{137}Cs	^{40}K
^{226}Ra	**0.823**			
^{137}Cs	**0.642**	**0.686**		
^{40}K	**0.837**	**0.788**	**0.596**	
^{232}Th	**0.823**	**0.732**	0.548	**0.682**

Bold face numbers are significant at the 95 % confidence level

Table 4. Pearson correlation coefficients between the radionuclide activities and the percentages of the grain size fractions and the general composition of the sediments in the cores Y1, Y2 and profile Y3 retrieved in the Yesa Reservoir.

		clay	silt	sand	OM	$CO_3^=$	residual
					%		
core Y1	^{210}Pb	0.200	0.365	-0.343	0.186	-0.296	0.276
	^{226}Ra	0.076	0.254	-0.221	**0.571**	-0.275	0.212
	^{137}Cs	0.094	-0.021	-0.011	**-0.500**	**-0.588**	**0.646**
	^{40}K	**0.459**	0.412	**-0.455**	0.097	**-0.518**	**0.509**
	^{232}Th	0.170	**0.503**	-0.443	0.376	**-0.466**	0.425
	^{238}U	0.000	0.107	-0.083	0.156	0.123	-0.141
core Y2	^{210}Pb	0.315	0.512	-0.470	-0.296	0.341	-0.298
	^{226}Ra	0.535	0.529	**-0.554**	0.330	**-0.587**	0.546
	^{137}Cs	0.227	0.124	-0.164	0.247	0.136	-0.186
	^{40}K	**0.784**	**0.579**	**-0.672**	0.457	-0.430	0.361
	^{232}Th	**0.586**	**0.611**	**-0.630**	**0.568**	-0.463	0.374
	^{238}U	0.217	-0.132	0.023	-0.467	0.210	-0.131
profile Y3	^{210}Pb	**0.591**	**0.654**	**-0.662**	**0.740**	**-0.881**	**0.810**
	^{226}Ra	**0.642**	**0.637**	**-0.670**	0.496	**-0.757**	**0.792**
	^{137}Cs	0.313	0.174	-0.236	0.388	-0.487	0.462
	^{40}K	**0.876**	**0.742**	**-0.830**	**0.818**	**-0.920**	**0.813**
	^{232}Th	0.493	**0.638**	**-0.614**	**0.557**	**-0.712**	**0.682**

Bold numbers are significant at the 95 % confidence level

Table 5. Basic statistics of the contents of stable elements (mg kg^{-1}) analyzed in the sediments of profile Y3 and cores Y1 and Y2 in the Yesa Reservoir

		Ca	Al	Fe	K	Na	Mg	Mn	Sr	Ba	Li	Pb	Zn	Cr	Ni	Cu	Co	Cd
Y1	mean	100894	22588	17643	10436	4920	3567	392.9	346.1	229.7	73.8	85.2	50.7	5.0	1.8	1.6	1.6	bdl
	median	101110	22878	18604	10907	4684	3594	402.4	349.0	179.1	74.8	86.8	51.5	5.3	1.8	1.4	1.6	bdl
	sd	13270	4079	2449	2072	1350	616	42.3	29.7	131.5	8.5	11.6	8.5	1.1	0.4	0.5	0.2	bdl
	min	72437	10866	11450	4493	3528	2088	263.6	259.6	57.2	50.0	51.0	26.1	2.0	1.0	1.1	1.1	bdl
	max	130565	31392	20374	14090	9718	4885	460.7	406.5	594.6	85.7	108.9	61.3	6.3	2.9	2.7	1.9	bdl
Y2	mean	105266	25086	18244	9781	6943	3815	436.7	353.9	479.2	84.9	81.1	65.3	4.5	2.5	1.6	0.5	bdl
	median	104179	26035	18006	9592	6923	3638	410.6	356.9	366.4	89.0	82.5	53.0	4.4	2.6	1.8	0.6	bdl
	sd	13175	2976	2238	1912	1045	532	68.3	27.6	284.0	10.9	9.9	33.0	1.0	0.5	0.4	0.2	bdl
	min	83922	18834	14236	6276	4797	3156	365.5	307.1	246.6	66.4	57.9	37.7	2.8	1.6	0.9	0.1	bdl
	max	130543	28930	22423	12681	9175	4812	598.4	408.9	1082.1	99.1	92.9	139.5	6.0	3.3	2.1	0.7	bdl
Y3	mean	89239	26161	18144	10661	9554	4007	375.7	258.1	216.9	82.3	33.9	52.3	56.9	26.6	14.7	9.9	1.9
	median	90700	25900	17800	10600	9505	3880	376.0	257.5	221.5	81.0	34.7	52.8	58.6	26.4	13.8	10.4	1.4
	sd	9281	3089	2183	1750	1372	657	28.8	19.2	34.8	9.4	6.8	8.3	9.9	3.8	4.6	1.6	2.1
	min	70600	18900	14900	7730	7180	2700	296.0	220.0	166.0	67.7	16.3	41.2	42.2	20.6	12.0	6.6	0.8
	max	105000	31300	22100	13400	13100	5170	411.0	301.0	279.0	94.1	43.2	63.6	69.3	31.0	32.1	12.1	10.0

sd : standard deviation
bdl: below detection level

Table 6. Pearson correlation coefficients between the radionuclide activities (Bq kg^{-1}) and contents of stable elements (mg kg^{-1}) in the sediments of the Yesa Reservoir.

		Mg	K	Na	Pb	Ba	Zn	Sr	Li	Mn	Co	Ni	Cu	Cr	Cd	Fe	Al	Ca
Y1	^{210}Pb	0.371	0.310	0.233	**0.464**	0.175	0.393	-0.056	**0.446**	0.278	**0.441**	0.349	0.342	0.345	0.080	0.204	**0.465**	-0.216
	^{226}Ra	**0.443**	**0.668**	-0.114	**0.701**	-0.189	**0.635**	-0.160	**0.700**	**0.649**	0.419	0.412	0.072	**0.698**	-0.070	**0.652**	**0.653**	-0.338
	^{137}Cs	0.268	**0.461**	-0.349	0.149	-0.198	**0.447**	**-0.625**	0.341	0.334	0.116	**0.474**	0.002	0.323	-0.209	0.161	0.115	**-0.690**
	^{40}K	**0.603**	**0.877**	-0.285	**0.800**	-0.118	**0.908**	**-0.512**	**0.886**	**0.738**	0.382	**0.700**	0.136	**0.895**	-0.286	**0.765**	**0.718**	**-0.678**
	^{232}Th	**0.536**	**0.702**	0.067	**0.720**	0.082	**0.694**	-0.259	**0.728**	**0.617**	0.407	**0.509**	0.185	**0.701**	-0.088	**0.536**	**0.698**	**-0.493**
	^{238}U	0.192	0.272	-0.228	0.242	0.019	0.394	-0.161	0.256	**0.511**	-0.036	0.268	0.278	**0.444**	-0.235	**0.496**	0.083	-0.288
Y2	^{210}Pb	**-0.596**	-0.003	0.314	-0.134	-0.230	**0.572**	-0.051	0.070	0.015	-0.111	-0.075	-0.119	-0.030	0.008	0.126	-0.043	0.065
	^{226}Ra	0.133	0.473	0.081	-0.006	0.296	0.412	-0.079	-0.192	0.471	-0.378	-0.042	-0.404	0.017	-0.415	-0.091	0.139	-0.471
	^{137}Cs	0.331	0.079	0.065	0.032	0.443	-0.334	**0.680**	**0.712**	-0.493	**0.660**	**0.625**	**0.643**	0.465	**0.687**	0.145	0.211	0.268
	^{40}K	0.443	**0.714**	-0.279	0.424	0.178	0.206	-0.060	0.221	0.468	-0.014	0.373	0.046	0.539	-0.152	0.364	0.531	-0.481
	^{232}Th	0.252	**0.558**	-0.040	0.379	0.215	0.064	-0.113	0.172	0.316	0.008	0.312	0.039	0.430	-0.106	0.302	0.479	-0.545
	^{238}U	0.204	0.324	-0.233	0.422	0.006	-0.344	0.295	**0.671**	-0.142	**0.604**	**0.640**	0.503	0.501	0.484	0.277	0.284	0.048
Y3	^{210}Pb	**0.580**	**0.729**	-0.374	0.394	**-0.520**	**0.602**	0.044	**0.669**	**0.528**	0.425	**0.622**	-0.209	**0.572**	-0.364	0.359	**0.577**	**-0.519**
	^{226}Ra	**0.674**	**0.695**	-0.350	0.523	0.457	-0.469	**0.540**	0.122	**0.630**	0.453	0.454	**0.568**	-0.030	**0.530**	-0.270	0.376	**0.660**
	^{137}Cs	0.439	0.401	-0.056	0.079	-0.047	-0.218	0.126	0.285	0.273	0.160	-0.073	0.195	-0.185	0.075	-0.229	-0.096	0.313
	^{40}K	0.717	**0.872**	-0.301	**0.689**	0.481	**-0.631**	**0.784**	0.122	**0.831**	0.505	0.518	**0.772**	-0.130	**0.738**	-0.209	0.543	**0.783**
	^{232}Th	0.492	**0.687**	-0.443	0.422	0.360	-0.419	0.502	0.035	**0.607**	**0.577**	0.387	**0.553**	-0.221	**0.523**	-0.390	0.338	0.475

Bold numbers are significant at the 95 % confidence level

Table 7. Basic statistics of the $^{238}U/^{226}Ra$ and $^{232}Th/^{226}Ra$ ratios in the cores Y1, Y2 and profile Y3 retrieved in the Yesa Reservoir.

	Core Y1		Core Y2		Profile Y3
	$^{238}U/^{226}Ra$	$^{232}Th/^{226}Ra$	$^{238}U/^{226}Ra$	$^{232}Th/^{226}Ra$	$^{232}Th/^{226}Ra$
mean	1.57	1.39	1.0	1.2	1.1
median	1.59	1.39	0.96	1.17	1.17
sd	0.31	0.13	0.2	0.1	0.1
min	1.00	1.22	0.7	1.0	0.8
max	2.29	1.71	1.5	1.3	1.3

sd: standard deviation